Journal of Electroceramics 6:2, 101–108, 2001

Effect of Nb Doping on (Sr,Ba)TiO_3 (BST) Ceramic Samples

S. GARCÍA,[1,2] R. FONT,[1] J. PORTELLES,[1,2] R.J. QUIÑONES,[1] J. HEIRAS[2] & J.M. SIQUEIROS[2]
[1]*Facultad de Física, Universidad de La Habana, San Lázaro y L, 10400, La Habana, Cuba*
[2]*Centro de Ciencias de la Materia Condensada, UNAM, Apartado Postal 2681, Ensenada, B.C, México*

Submitted March 31, 2000; Revised October 17, 2000; Accepted October 19, 2000

Abstract. The effect of doping the $Sr_{0.3}Ba_{0.7}Ti_{(1-5y/4)}Nb_yO_3$ ceramic with different concentration of Nb is studied by scanning electron microscopy (SEM), X-ray diffraction and thermoelectric analysis. It is observed that the grain size decreases as the Nb concentration increases. The critical temperature T_c has a linear decrease at a rate of 19°C/mol% of Nb. The temperature dependence of the dielectric permittivity presents strongly broadened curves, which suggest a non Curie-Weiss behavior near the transition temperature. The diffuse phase transition coefficient (δ) was also determined and its value leads to the conclusion that the degree of disorder in the system increases with the presence of the Nb cation.

Keywords: cation substitution, dielectric permittivity, SBT ceramics, diffuse phase transition

Introduction

Doping with isovalent or aliovalent ions of the A or B sites of the ABO_3 perovskite system is a widely used procedure to modify the relevant properties of the ceramic such as dielectric permittivity, dielectric losses, pyroelectric coefficient, critical temperature, etc. A good example is the doping of $BaTiO_3$ or $BaTiO_3$ based ceramics [1–3].

In particular, the $Sr_xBa_{1-x}TiO_3$ (BST) system has attracted attention due to its many potential application in devices such as capacitors, phase shifting in antenna and radar equipment, ferroelectric memory for computers and many more [4, 5]. Doping of BST to fine tune its properties for particular applications is therefore an interesting line of research.

Doping of the $Sr_{0.4}Ba_{0.6}TiO_3$ (BST40) and $Sr_{0.3}$-$Ba_{0.7}TiO_3$ (BST30) compositions with different elements is particularly attractive because of the high dielectric permittivity, low losses and transition temperatures close to room temperature of the undoped system. For example, it is known that when the $Sr_{0.4}Ba_{0.6}TiO_3$ (BST40) ceramic samples are doped in their B site, their dielectric properties will strongly depend on the particular dopant and Nb^{5+} is one of the most commonly used for the above mentioned composition [6–8]. However, as far as we know, the effect of doping on the dielectric properties of BST30 has not been thoroughly investigated [9]. For this reason, the present work is dedicated to the study of the influence of different amounts of Nb^{5+} doping on the dielectric properties of $Sr_{0.3}Ba_{0.7}TiO_3$ (BST30) ceramics.

Experimental

The composition of the samples under study are given by $Sr_{0.3}Ba_{0.7}Ti_{(1-5y/4)}Nb_yO_3$ where $y = 0$, 0.01, 0.05 and 0.1. The samples were prepared by the traditional ceramic method [10] by mixing high purity $SrCO_3$, $BaCO_3$, TiO_2 and Nb_2O_5 in an agate mortar for 2 hours, die-pressed into 22 mm diameter, 10 mm thick tablets and then calcined for 2 hours at 1100°C in open air. The tablets were crushed and milled again for 3 hours. The resulting powders were die-pressed into 10 mm diameter, 1mm thick disks and sintered at 1350°C for 4 hours.

A qualitative X-ray diffraction (XRD) analysis was performed afterward to determine the presence of different phases in the samples. For such study, a PHILIPS PW-1710 with Cu anode ($\lambda_{k\alpha 1} = 1.54056$ Å

and $\lambda_{k\alpha 2} = 1.54439$ Å) at 40 kV and 30 mA was used. For grain-size analysis, Scanning Electron Microscopy (SEM) was performed in fractured samples using a 10 kV JEOL microscope model M5400. The dielectric permittivity dependence with temperature was measured with a RLC bridge by Philips model PM632, at 1 kHz.

Results and Discussion

Due to the similar electronegativity and ionic radii of the Nb^{5+} and Ti^{4+} ions, it may be assumed that the Nb^{5+} ion will occupy the B sites in the perovskite structure. The Ti^{4+} for Nb^{5+} substitution will therefore introduce an excess positive charge and electrical neutrality will demand the presence of Ti vacancies. A better chemical representation of the doped ceramic will be given by the formula $Sr_{0.3}Ba_{0.7}Ti_{(1-5y/4)}V_{y/4}Nb_yO_3$ where V represents Ti vacancies.

XRD analysis showed the samples to be isostructural with BST with very little or no second phases present.

SEM micrographs corresponding to fractured $Sr_{0.3}Ba_{0.7}TiO_3 (y = 0)$ samples are presented in Fig. 1

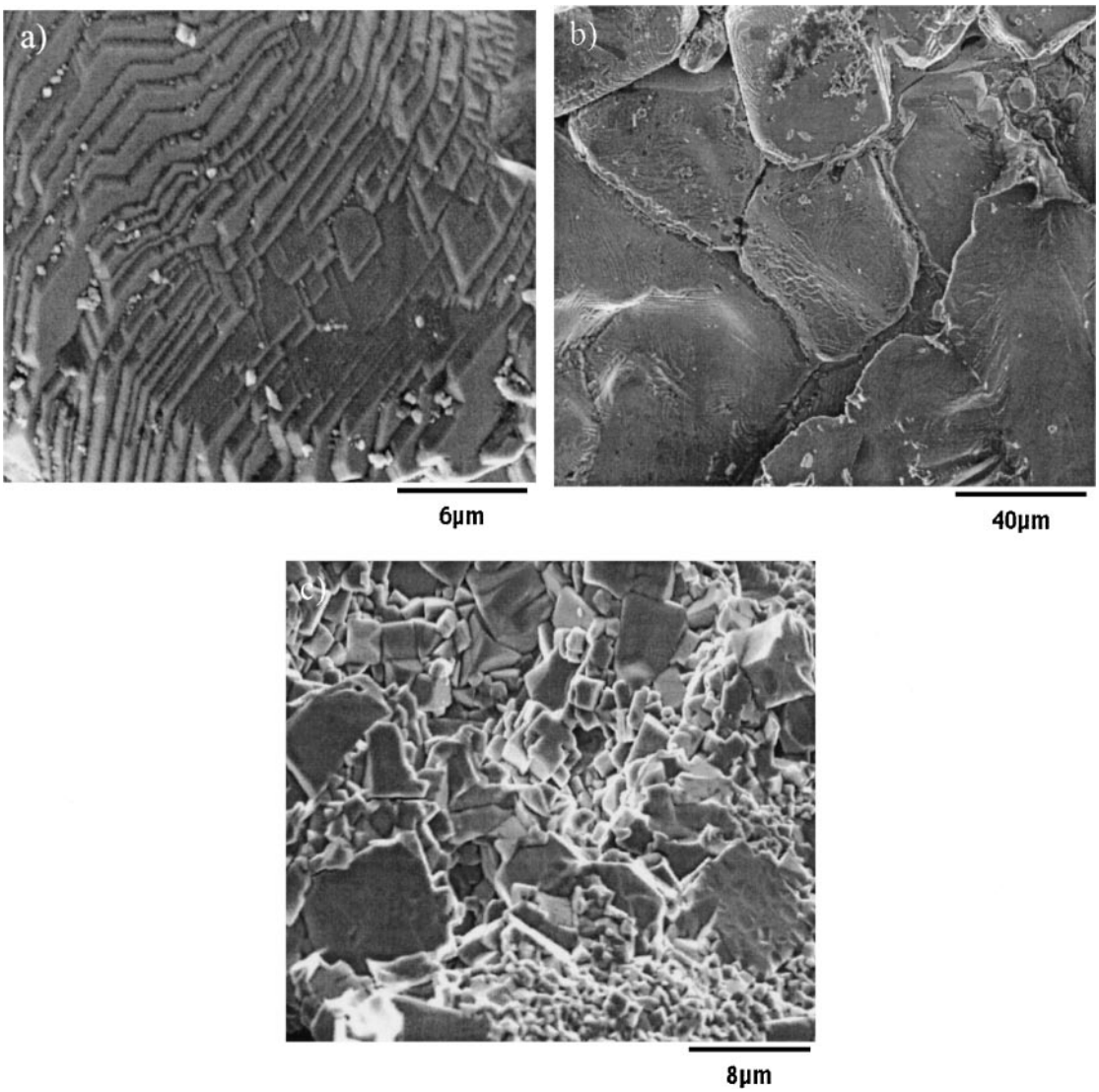

Fig. 1. SEM micrographs of the $Sr_{0.3}Ba_{0.7}TiO_3$ sample sintered at 1350°C for 4 hours.

A duplex or bimodal grain size distribution showing large grains in a small grain matrix is presented on Fig. 2(c). Kolar et al. [11] state that during the sintering process of BST Ba^{2+} ions move faster than Sr^{2+} ions resulting in Ba and Ti rich regions favoring the formation of a polytitanate ($Ba_6Ti_{17}O_{40}$) which, at temperatures around 1280–1300°C, forms an eutectic with $BaTiO_3$. The grain distribution pattern and the fingerprint-like topography of the large particles indicates a liquid phase assisted grain growth during the sintering process where surface melting occurs at isolated points of the sample volume [12].

Table 1 condenses the grain size information corresponding to the different compositions. Figure 2 presents the SEM micrographs for the $y = 0.01$, 0.05 and 0.1 compositions.

From the values presented in Table 1 and the micrographs of Fig. 2 it is possible to observe a decrease in grain size with the increase on Nb concentration in the samples.

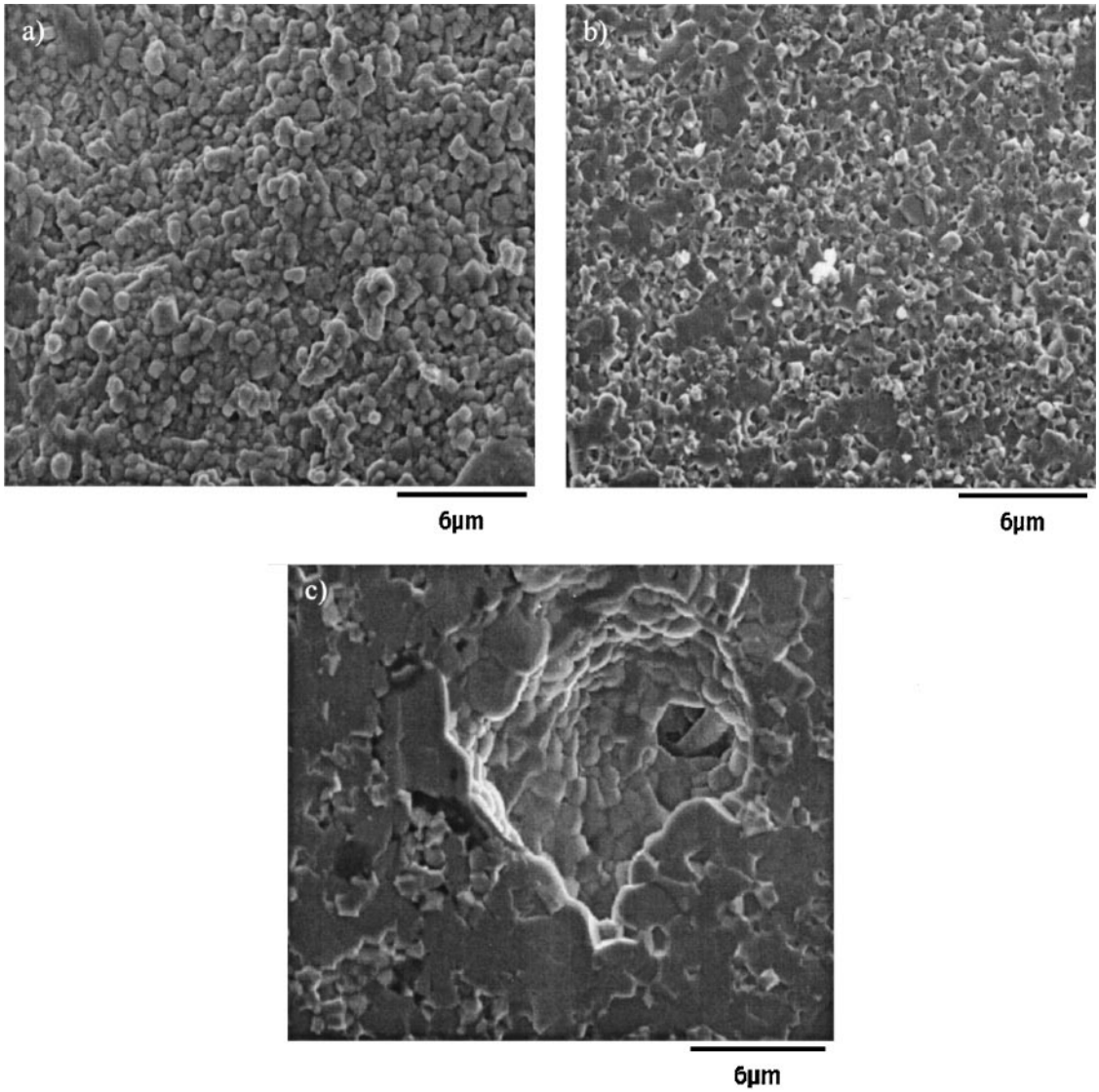

Fig. 2. SEM micrographs of the $Sr_{0.3}Ba_{0.7}Ti_{(1-5y/4)}Nb_yO_3$ samples sintered at 1350°C for 4 hours for (a) $y = 0.01$, (b) $y = 0.05$ and (c) $y = 0.1$.

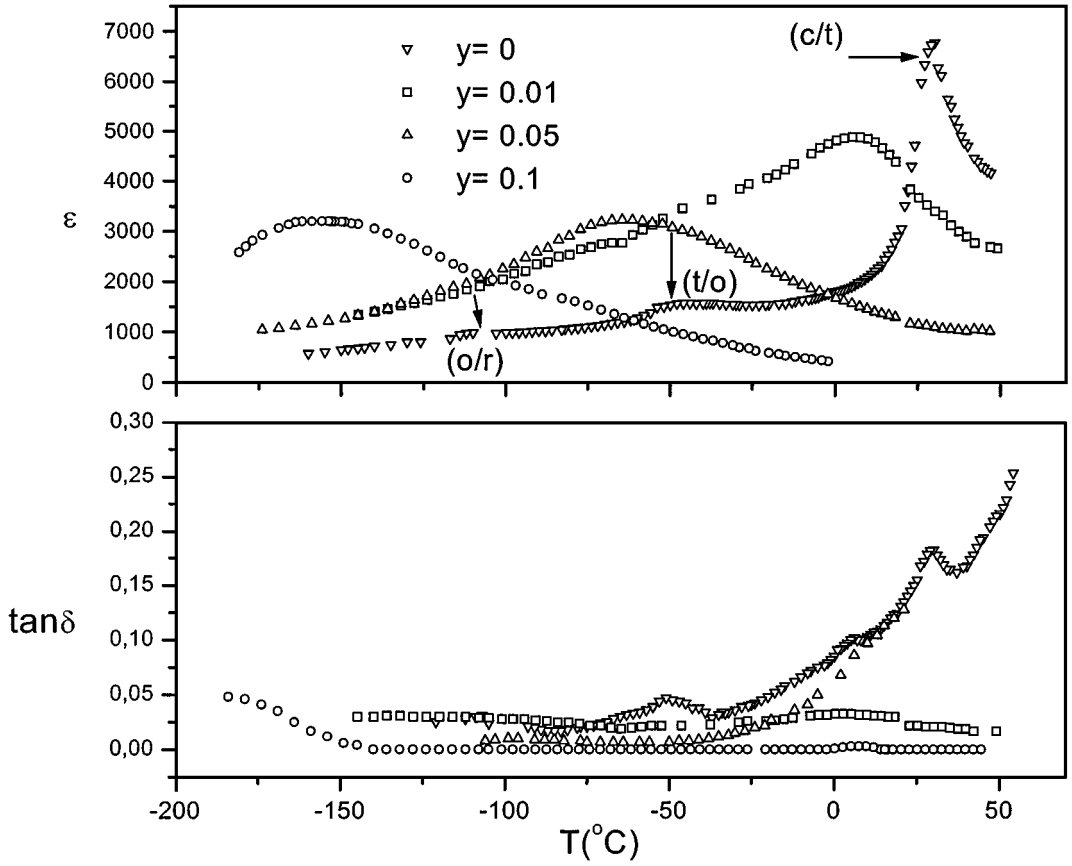

Fig. 3. Dependence of the permittivity and dielectric losses with temperature $y = 0, 0.01, 0.05$ and 0.1 compositions of the or the $Sr_{0.3}Ba_{0.7}Ti_{(1-5y/4)}Nb_yO_3$ ceramic system.

Considering the findings of Chen et al. [1], relative to the mechanism of grain growth inhibition in highly donor-doped $BaTiO_3$, the fact that for this air-fired samples niobium acts as a powerful grain growth inhibitor when added in concentrations of $\leq$0.5 mol%, is to be expected, in particular for the 0.01 and 0.05 BST doped samples. That is, grain size decrease is most likely related to Nb content and Ti vacancies. It is worth mentioning that no sign of a liquid phase was found in these cases in any stage of the sintering process.

Table 1. Grain sizes for the $Sr_{0.3}Ba_{0.7}Ti_{(1-5y/4)}Nb_yO_3$ samples with $y = 0, 0.01, 0.05$ y 0.1.

Composition	Large grains (μm)	Small grains (μm)
0	8	1
0.01	–	0.61
0.05	–	0.55
0.1	–	0.50

Figure 3 shows the dependence of the permittivity and the dielectric losses with temperature measured at 1 kHz for all the studied compositions. In the curve corresponding to BST30 ($y = 0$), the characteristic crystalline phase transitions that this system presents as the temperature is decreased, that is, cubic-tetragonal (c/t), tetragonal-orthorhombic (t/o) and (orthohombic-rhombohedral (o/r), are indicated. The displacement toward higher temperatures shown by T_{max} corresponding to the t/o and o/r transitions for the samples doped with 1% Nb and the fact that the maxima corresponding to those transitions are not present in the 5% and 10% Nb lead us to think in a coalescence of the three phase transitions in the 5% y 1% Nb doped compositions, similar to the situation reported in [13]. A broadening of the c/t transition in the ε vs. T curves evidences a

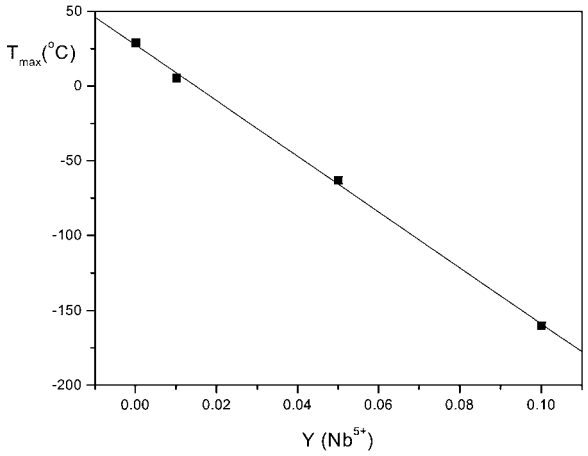

Fig. 4. Dependence of the transition temperature (T_{max}) with Nb concentration.

growing departure from a Curie-Weiss behavior with the increase in Nb concentration, close to the transition temperature. In contrast to the behavior of the $Sr_{0.3}Ba_{0.7}TiO_3$ ($y = 0$) composition where the temperatures for the dielectric permittivity T_{max} and dielectric losses maxima T_{dl} nearly coincide, in the Nb doped samples T_{max} is higher than T_{dl} and the difference between them grows as the Nb concentration increases. Such behavior suggests a change in the type of transition that the BST30 system undergoes when doped with Nb.

Figure 4 shows a fast decrease of T_{max} as a function of Nb concentration of the order of 19°C/mol%, much faster than the value of 3,75°C/mol% reported in the literature for BST [14].

The inverse permittivity curves against temperature for compositions $y = 0.01, 0.05, 0.1$, taken at 1 kHz, are presented in Fig. 5. According to the method reported by Cross [15]. The curves were divided in three regions

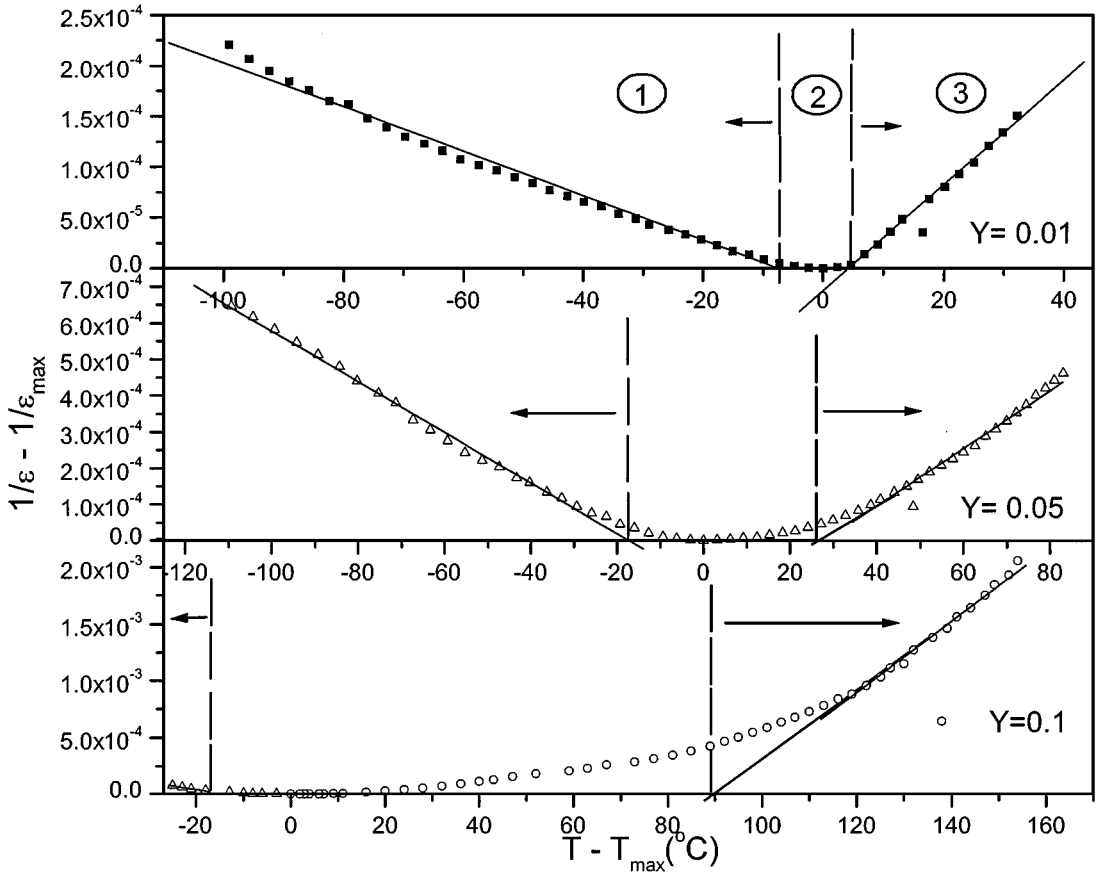

Fig. 5. Dependence of the inverse permittivity with ($T - T_{max}$) for the $Sr_{0.3}Ba_{0.7}Ti_{(1-5y/4)}Nb_yO_3$ ceramic system with $y = 0.01, 0.05, 0.1$.

labeled 1, 2, 3. Region 1 corresponds to the ferroelectric phase. Here, by linearly extrapolating the experimental points to the temperature axis, the Curie Temperature (T_c) for this material is obtained. Region 2 is the part of the curve close to the transition temperature evidencing a diffuse phase transition up to T_0, while region 3 shows the linear behavior of $1/\varepsilon$ with temperature following a Curie-Weiss law. The Curie-Weiss temperature (T_{cw}) is found also by extrapolation of the experimental data to the temperature axis. The difference between the Curie-Weiss temperature and the Curie temperature (ΔT) is characteristic of the nature of the paraelectric-ferroelectric phase transition. In these ceramics ΔT tends to increase with Nb concentration indicating an enhancement of the diffuse character of the transition. For the paraelectric phase, it was possible to show that the inverse permittivity follows a $(T - T_{max})^2$ law. The diffuseness coefficient δ associated to the cationic disorder of the system was determined using the quadratic expression proposed by Smolienskii [16, 17]:

$$1/\varepsilon - 1/\varepsilon_{max} = B(T - T_m)^2 \qquad (1)$$

where

$$B = 1/2\varepsilon_{max}\delta^2$$

This dependence is presented in Fig. 6(a) for the $y = 0.05$ composition. The slope of the line obtained from the linear regression of the data corresponds to B in Eq. (1). The diffuseness coefficient δ obtained from this value is also presented in Fig. 6(a). Uchino and Nomura [18], reported that not all diffuse phase transitions obey

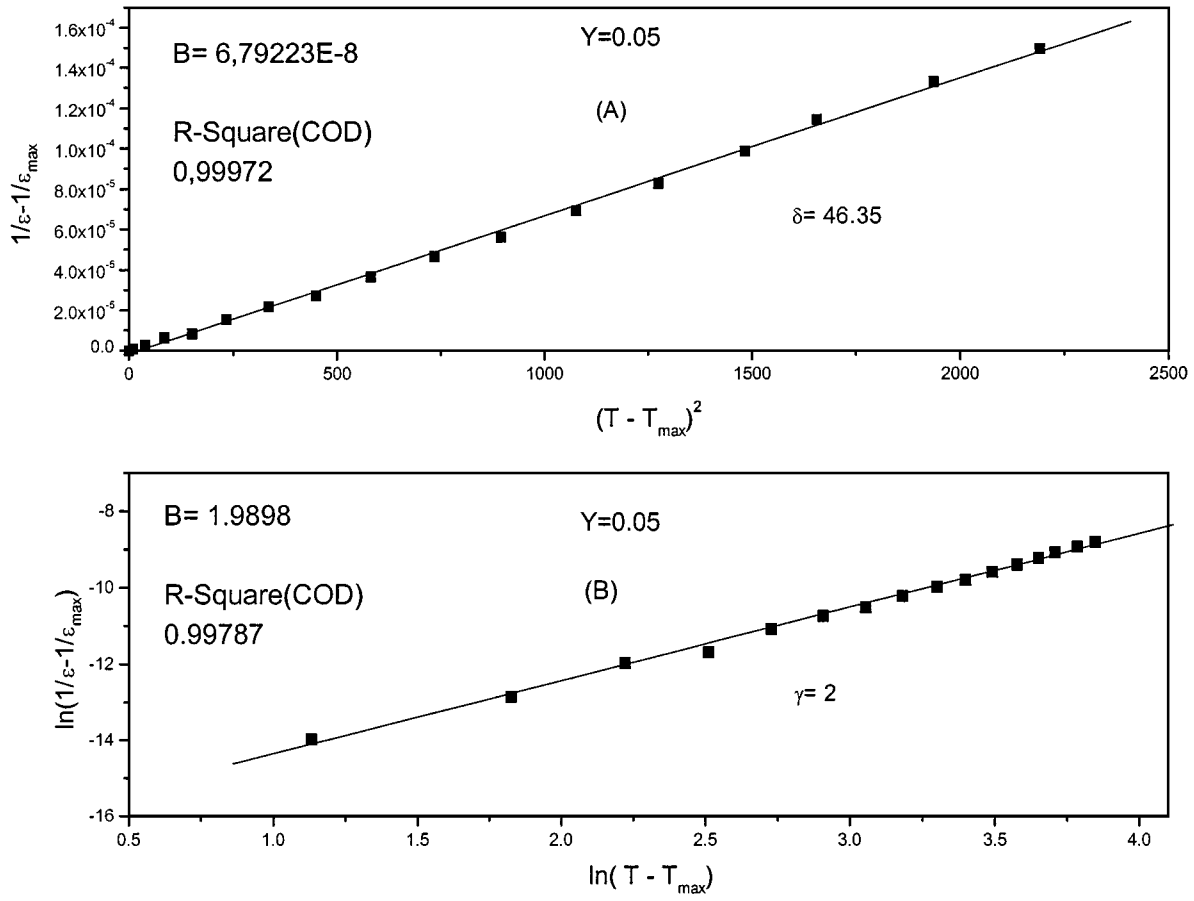

Fig. 6. Dependence of (a) inverse permittivity with $(T - T_{max})^2$ and (b) $\ln(1/\varepsilon\ 1/\varepsilon_{max})$ vs. $\ln(T - T_{max})$ for the $Sr_{0.3}Ba_{0.7}Ti_{(1-5y/4)}Nb_yO_3$ ($y = 0.05$) sample.

Table 2. Curie temperature (T_c), Curie-Weiss Temperature (T_{cw}), $\Delta T = (T_c - T_{cw})$ and diffuse phase transition coefficient (δ) for the $Sr_{0.3}Ba_{0.7}Ti_{(1-5y/4)}Nb_yO_3$ samples with $y = 0.01, 0.05, 0.1$.

Y	T_c (°C)	T_{cw} (°C)	ΔT (°C)	δ
0.01	−1.59	10.33	11.92	23.54
0.05	−83.37	−38.83	44.54	46.35
0.1	−173.93	−67.33	106.60	48.33

exactly Smolienskii's relation, and developed a more general expression:

$$1/\varepsilon - 1/\varepsilon_{max} = (T - T_{max})^{\gamma}/c' \qquad (2)$$

where C' and γ are constants and $1 \leq \gamma \leq 2$. The limiting values of γ lead to Curie-Weiss law, for $\gamma = 1$, and Smolenskii's quadratic expression, for $\gamma = 2$. The plot of $\ln(1/\varepsilon - 1/\varepsilon_{max})$ vs. $\ln(T - T_m)$ for the $y = 0.05$ sample shown in Fig. 6(b) allows the determination of γ for this composition. Using linear regression of the data, a value of 2 was found for γ, in good agreement with the result shown in Fig. 6(a). The values of T_c, T_{cw}, $\Delta T = (T_{cw} - T_c)$ and δ are presented in Table 2. From these data, the increment of the value of δ with Nb content is evident and in good agreement with the diminishing of the grain size in the samples as discussed by Uchino [19]. A possible explanation of this behavior may be attributed to the enhancement in the degree of disorder having two ions to occupy the same lattice site. Neighboring domains will then have different compositional order regarding the positions of the ions in the lattice sites giving rise to a broad transition temperature distribution instead of narrow one designated as Curie Temperature. Cationic disorder in the lattice also affects long range interactions resulting in a weaker ferroelectric state and a lower transition temperature. In summary, cationic disorder not only broadens the transition temperature distribution but also shifts its maxima toward lower temperatures. Furthermore, the substitution of Ti^{4+} by Nb^{5+} will produce vacancies in the crystal structure that will grow in number with Nb content, contributing also to disorder in the ceramic structure.

Conclusions

A monophasic $Sr_{0.3}Ba_{0.7}Ti_{(1-5y/4)}Nb_yO_3$ compound is obtained isostructural with BST up to 10% Nb concentration. A notable difference is observed in the grain size distribution between the non-doped samples and those with different concentrations of Nb. Bimodal or duplex grain-size distributions are not observed with the incorporation of the Nb ion to the crystalline structure. No liquid phase is detected in the Nb doped samples and the grain size decreases with increasing Nb doping. A linear behavior of the transition temperature (T_{max}) with Nb concentration is observed decreasing at a rate of 19°C/mol% for the range of compositions studied. The dielectric losses decrease and the transition becomes more diffuse with Nb concentration. This behavior may be attributed to the enhancement in the degree of disorder having two ions to occupy the same lattice site. This disorder not only broadens the transition temperature distribution but also shifts its maxima toward lower temperatures.

Acknowledgments

This work was partially sponsored by CoNaCyT Proj. No. 33586E and DGAPA Proj. No. IN104000. S. García thanks DGIA-UNAM for its financial support.

Thanks are due to E. Aparicio and I. Gradilla, for their technical help.

References

1. H.M. Chan, M.P. Harmer, and D.M. Smyth, *J. Am. Ceram. Soc.*, **69**(6), 507 (1986).
2. H. Kishi, N. Kohzu, Y. Mizuno, Y. Iguchi, and J. Sugino, *Jpn. J. Appl. Phys.*, **83**, 5452 (1999).
3. M. Drofenik, A. Popovi, and D. Kolar, *Ceramic Bulletin*, **63**(5), 702 (1984).
4. L. Zhang, W.L. Zhong, and G. Wamg, *Sold State Comm.*, **10**(12), 761 (1998).
5. S. Zafar, P. Chu, T. Remmel, R.E. Jones, B. White, D. Gentile, B. Jiang, B. Melnick, D. Taylor, P. Zucher, and S. Gillespie, *Mat. Res. Soc. Symp. Proc.*, **43**, 15 (1998).
6. S.B. Herner, F.A. Selmi, V.V. Varandan, and V.K. Varandan, *Materials Letters*, **15**, 317 (1993).
7. T. Ishiya, S. Tashiro, and H. Igarashi, *Jpn. J. Appl. Phys.*, **34**, 5309 (1995).
8. T. Yamamoto and S. Takao, *Jpn. J. Appl. Phys.*, **31**, 3120 (1992).
9. J. Joseph, T.M. Vimala, K.C. James, and V.R.K. Murthy, *Jpn. J. Appl. Phys.*, **35**, 179 (1995).
10. A.T. Ring, *Fundamental of Ceramic Powder Processing and Synthesis* (Academic Press, 1998).
11. D. Kolar, M. Trontell, and Z. Stadller, *J. Am. Ceram. Soc.*, **65**, 10 (1982).
12. M.R. German, *Liquid Phase Sintering* (Plenum Press, New York, 1985).

13. F.D. Morrison, D.C. Sinclair, and A.R. West, *J. Appl. Phys.*, **86**(11), 6355 (1999).
14. F.S. Galasso, *Structure and Preparation of Perovskite-Type Compounds* (Pergamon Press, London, 1969).
15. L.E. Cross, *Ferroelectrics*, **76**, 241 (1987).
16. G.A. Smolenskii, V.A. Isupov, and A.I. Agranovskaya, *Soviet Physics–Solid State*, **2**(11), 2584 (1960).
17. V.V. Kirilov and V.A. Isupov, *Ferroelectric*, **5**, 3 (1973).
18. K. Uchino and S. Nomura, *Ferroelectric Lett. Sect*, **44**, 55 (1982).
19. K. Uchino, *Ferroelectric Devices* (Marcel Dekker, Inc, New York, 2000).